Contribution from the Department of Chemistry, Box 8204, North Carolina State University, Raleigh, North Carolina 27695

Studies of Electrocatalytic DNA Cleavage by Oxoruthenium(IV). X-ray Crystal Structure of $[Ru(tpy)(tmen)OH_2](ClO_4)_2$ (tmen = *N,N,N',N'*-Tetramethylethylenediamine; tpy = 2,2',2''-Terpyridine)

Neena Grover, Nishi Gupta, Phirtu Singh, and H. Holden Thorp*

Received July 17, 1991

The interactions of $Ru^{II}(tpy)(bpy)OH_2^{2+}$ (**1**), $Ru^{II}(tpy)(phen)OH_2^{2+}$ (**2**), and $Ru^{II}(tpy)(tmen)OH_2^{2+}$ (**3**) (tpy = 2,2',2''-terpyridine, bpy = 2,2'-bipyridine, phen = 1,10-phenanthroline, tmen = *N,N,N',N'*-tetramethylethylenediamine) with DNA have been investigated by cyclic voltammetry. The addition of DNA to solutions of these complexes causes a dramatic decrease in current for the Ru(IV/III) and Ru(III/II) couples indicative of binding of the complexes to DNA. From the decrease in current, binding constants 15×10^3 M^{-1}, 78×10^3 M^{-1}, and 5.3×10^3 M^{-1} can be estimated for **1**-**3**, respectively. Thus, the binding affinity appears to be partly a function of the extended planarity and aromaticity of the bidentate ligands. The previously reported activity of the Ru(IV) state toward DNA cleavage is apparent as a current enhancement in the Ru(IV/III) oxidation wave. As a result of the differential binding affinity of **1** and **2**, greater electrocatalytic efficiency for DNA cleavage is observed for **1** upon controlled potential electrolysis at 0.8 V. A single crystal of $3(ClO_4)_2$ suitable for X-ray diffraction was also obtained. X-ray data: $C_{21}H_{29}N_5O_9RuCl_2$, monoclinic, $P2_1/c$, $a = 15.314$ (5) Å, $b = 10.754$ (4) Å, $c = 16.150$ (8) Å, $\beta = 96.99$ (3)°, $V = 2640$ (2) Å^3, $Z = 4$, $R = 0.0699$, and $R_w = 0.0718$ for 3601 reflections with $I > 2\sigma(I)$. The electronic properties of **2** and **3** are also reported.

The electrochemistry of certain polypyridyl complexes that bind to DNA has been studied in detail.[1-3] Bard and co-workers have examined by cyclic voltammetry the binding to DNA of the complexes $Co(phen)_3^{3+/2+}$ and $Fe(phen)_3^{3+/2+}$ (phen = 1,10-phenanthroline), which do not react with DNA in either redox state in the absence of light.[4] Analysis of the peak currents and potentials provides detailed information on the binding of the complexes to the DNA. In an early communication, these workers suggested that it might be possible to induce strand scission by electrochemical activation of an appropriate metal complex.[1] We report here on cyclic voltammetry studies on such a system.

We have recently demonstrated that the oxoruthenium(IV) complex $Ru^{IV}(tpy)(bpy)O^{2+}$ is an efficient DNA cleavage reagent (bpy = 2,2'-bipyridine, tpy = 2,2',2''-terpyridine).[5] The cleavage reaction can be performed either by treatment of DNA with the active oxo form or by electrolysis at 0.8 V of DNA with the $Ru^{II}(tpy)(bpy)OH_2^{2+}$ form, which is converted by electrolysis to the oxo form via the reactions shown in eqs 1 and 2.[6] At pH 7,

$$Ru^{II}(tpy)(bpy)OH_2^{2+} \rightleftharpoons Ru^{III}(tpy)(bpy)OH^{2+} + e^- \quad (1)$$

$$Ru^{III}(tpy)(bpy)OH^{2+} \rightleftharpoons Ru^{IV}(tpy)(bpy)O^{2+} + e^- \quad (2)$$

$E_{1/2}$ for eq 1 is 0.49 V (SSCE) and 0.62 V for eq 2. No detectable cleavage is observed upon electrolysis of the DNA without catalyst or upon treatment with the Ru(II) form; however, incubation with $Ru^{IV}(tpy)(bpy)O^{2+}$ induces efficient strand scission.[5] The electrochemical reaction has been shown to be catalytic: under stoichiometric conditions, optical spectra show that $Ru^{IV}(tpy)(bpy)O^{2+}$ is converted *quantitatively* to $Ru^{II}(tpy)(bpy)OH_2^{2+}$ concomitant with DNA cleavage. Thus, the catalytic cycle shown in Scheme I has been conclusively demonstrated. The catalysis should therefore be evident in cyclic voltammetry studies of the cleavage reaction, an issue we will address in detail here.

In this report we will present initial studies on the cyclic voltammetry of $Ru^{II}(tpy)(bpy)OH_2^{2+}$ (**1**), $Ru^{II}(tpy)(phen)OH_2^{2+}$ (**2**), and $Ru^{II}(tpy)(tmen)OH_2^{2+}$ (**3**) in the presence of DNA (models of the complexes under study are shown in Figure 1). Cyclic voltammetry can be used to detect the binding of the complexes to DNA and shows that the phen complex binds appreciably more strongly than the bpy and tmen complexes, as expected on the basis of studies of related tris(polypyridyl) complexes.[1,2,7] The cleavage of DNA by the $Ru^{IV}O^{2+}$ forms, which has been detected by optical spectroscopy and gel electrophoresis,[5] is evident in the voltammograms obtained in the presence of DNA, and the different efficiencies of electrocatalytic cleavage can be understood in terms of the relative binding affinity of the complexes.

Scheme I

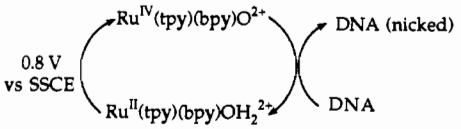

Experimental Section

$[Ru^{II}(tpy)(bpy)OH_2](ClO_4)_2$ (**1**) was prepared by a literature method.[6] $[Ru^{II}(tpy)(phen)OH_2](ClO_4)_2$ (**2**) was prepared by substitution of phen for bpy in the same procedure to yield a complex that gave satisfactory elemental analysis.

The general procedure used for the synthesis of $Ru^{II}(tpy)(tmen)OH_2^{2+}$ (**3**) and its $Ru^{IV}O^{2+}$ form is similar to that of Meyer and co-workers for the syntheses of $Ru^{IV}(tpy)(bpy)O^{2+}$ and $Ru^{II}(tpy)(bpy)OH_2^{2+}$.[6] The procedure of Che and co-workers[8] does provide pure samples of **3** and its oxidized $Ru^{IV}O^{2+}$ form; however, we have found that single crystals of **3** suitable for X-ray analysis are obtained only through the following procedure. A 0.190-g (0.325-mmol) sample of $[Ru(tpy)(tmen)Cl](ClO_4)$[8] was dissolved in 20 mL of 3:1 acetone/water, and 0.067 g (0.325 mmol) of $AgClO_4$ was added. The AgCl precipitate was filtered off, and slow evaporation of the filtrate led to the precipitation of black crystals suitable for X-ray analysis of $[Ru^{II}(tpy)(tmen)OH_2](ClO_4)_2$ (0.12 g, 55% yield). Anal. Calcd for $C_{21}H_{29}N_5O_9RuCl_2$: C, 37.79; H, 4.38; N, 10.49. Found: C, 37.76; H, 4.34; N, 10.40. We have found that the $Ru^{IV}(tpy)(tmen)O^{2+}$ complex can be prepared either by Che's method[8] or by oxidation of **2** in aqueous solution with Cl_2 gas.

The structure of **3** was solved by the Patterson method. Block-diagonal least-squares refinement yielded $R = 0.0699$ and $R_w = 0.0718$ for 3601 reflections with $I > 2\sigma(I)$ measured on a Nicolet P3/F diffractometer up to $2\theta = 55°$ at 25 °C (Mo Kα radiation, $\lambda = 0.71073$ Å). $C_{21}H_{29}N_5O_9RuCl_2$: monoclinic, $P2_1/c$, $a = 15.314$ (5) Å, $b = 10.754$ (4) Å, $c = 16.150$ (8) Å, $\beta = 96.99$ (3)°, $V = 2640$ (2) Å^3, $Z = 4$, $d_{calcd} = 1.680$ g/cm^3, and μ(Mo Kα) = 8.42 cm^{-1}.

Cyclic voltammetry was performed using a PAR 273A potentiostat and PAR M270 software in a cell that has been described.[9] Tin-doped indium oxide working electrodes were obtained from the Donnelly Corp. and prepared by 15-min sonications in alconox, ethanol, and twice in water. Cleaned electrodes were equilibrated overnight in the buffer to be used in the experiment. This final equilibration was vital to obtaining

(1) Carter, M. T.; Bard, A. J. *J. Am. Chem. Soc.* **1987**, *109*, 7528.
(2) Carter, M. T.; Rodriguez, M.; Bard, A. J. *J. Am. Chem. Soc.* **1989**, *111*, 8901.
(3) Carter, M. T.; Bard, A. J. *Bioconjugate Chem.* **1990**, *1*, 257.
(4) Barton, J. K.; Raphael, A. L. *J. Am. Chem. Soc.* **1984**, *106*, 2466.
(5) Grover, N.; Thorp, H. H. *J. Am. Chem. Soc.* **1991**, *113*, 7030.
(6) Takeuchi, K. J.; Thompson, M. S.; Pipes, D. W.; Meyer, T. J. *Inorg. Chem.* **1984**, *23*, 1845.
(7) Pyle, A. M.; Rehmann, J. P.; Meshoyrer, R.; Kumar, C. V.; Turro, N. J.; Barton, J. K. *J. Am. Chem. Soc.* **1989**, *111*, 3051.
(8) Ho, C.; Che, C.-M.; Lau, T.-C. *J. Chem. Soc., Dalton Trans.* **1990**, 967.
(9) Willit, J. L.; Bowden, E. F. *J. Phys. Chem.* **1990**, *94*, 8241.

0020-1669/92/1331-2014$03.00/0

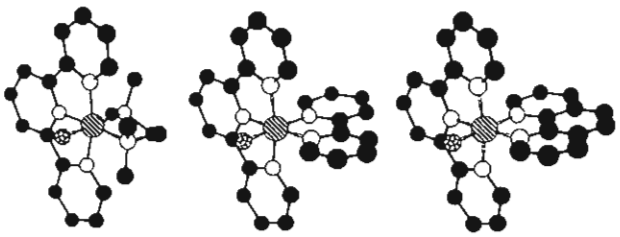

Figure 1. Models of complexes. Structures of **3** and **2** are based on the X-ray structures; the structure of **2** was generated by modification of the bpy ligand in the model of **1**.

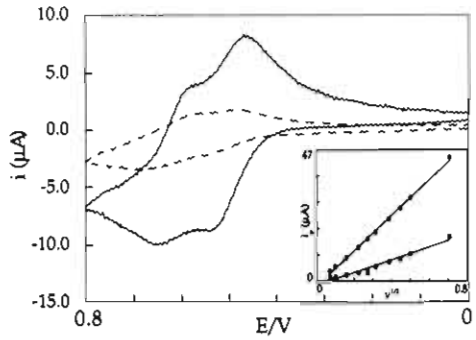

Figure 2. Cyclic voltammograms of 0.2 mM $[Ru^{II}(tpy)(bpy)OH_2](ClO_4)_2$ in 0.05 M phosphate buffer, pH 7, with (dashed line) and without (solid line) calf thymus DNA (7 mM nucleotide phosphate). Scan rate: 25 mV/s. Inset: Plot of $i_{pa}(Ru(III/II))$ vs $v^{1/2}$ in buffer (●, R = 0) and with DNA (■, R = 35, R = [DNA-nucleotide phosphate]/[metal complex]). Working electrode: ITO. Reference electrode: Ag/AgCl (1.0 M KCl). Couter electrode: Pt wire.

the quasi-reversible cyclic voltammograms described here. Edge-oriented pyrolytic graphite electrodes were a gift of Prof. E. F. Bowden and were prepared as described previously.[10] All measurements described here were performed in 50 mM phosphate buffer, pH 7.

Controlled potential electrolysis was performed in the same cell used for cyclic voltammetry. Solutions were diluted with bromphenol blue loading buffer and loaded onto 1% agarose gels and electrophoresed for 1 h at 44 V. The gels were stained with ethidium bromide and photographed under UV light. Calf thymus DNA was purchased from Sigma and used as described previously.[2] Plasmid pSport1 DNA was purchased from Bethesda Research Laboratories and used as received. Plasmid *φX174* DNA (rf I) was purchased from Pharmacia and used as received.

Results and Discussion

$Ru^{II}(tpy)(bpy)OH_2^{2+}$: Binding. The cyclic voltammogram of **1** using a tin-doped indium oxide (ITO) working electrode (Figure 2) shows two waves corresponding to $Ru^{III}(tpy)(bpy)OH^{2+}/Ru^{II}(tpy)(bpy)OH_2^{2+}$ ($E_{1/2}$ = 0.49 V vs Ag/AgCl) and $Ru^{IV}(tpy)(bpy)O^{2+}/Ru^{III}(tpy)(bpy)OH^{2+}$ ($E_{1/2}$ = 0.62 V).[6] The addition of calf thymus DNA causes a dramatic decrease in current, which is indicative of binding of the complex to the DNA.[1-3] This decrease arises because binding decreases the effective diffusion coefficient for the complex, and the observed current is proportional to the square root of the effective diffusion coefficient. This effect will be discussed in more detail below.

Extraction of binding information from the IV/III wave is difficult, because the $Ru^{IV}O^{2+}$ form is an efficient agent for the oxidation of DNA.[5] As we shall discuss below, the oxidation reaction causes significant changes in the peak morphology for the IV/III wave that complicate the effects of binding. We have observed by optical spectroscopy that the $Ru^{III}OH^{2+}$ form also oxidizes DNA but the rate is 1000 times slower,[11] too slow to affect measurements made on the cyclic voltammetry time scale. Thus, the binding studies we will now describe are based on the III/II couple. Also, we have observed by dialysis, ultrafiltration, and ethanol precipitation experiments covalent binding of the $Ru^{II}OH_2^{2+}$ complex to DNA,[11] presumably by replacement of the OH_2 ligand by nitrogen of a DNA heterocyclic base. The covalent binding is at a very low level, $r_b \sim 0.02$ or 1 Ru every 25 base pairs. The covalently bound material is not redox active in our potential window, because the stabilization of Ru(III) and Ru(IV) ordinarily brought about by deprotonation of the aqua ligand is no longer possible. Thus, the binding experiments described here monitor only noncovalently bound complexes, where the Ru(II)–OH_2 bond is still intact. Furthermore, we have determined $t_{1/2}$ for covalent binding to be >30 min, and the electrochemical experiments are performed immediately upon mixing of the complexes with DNA, well before appreciable covalent binding has occurred.

The peak current for the III/II couple (i_{pa}(III/II)) is a linear function of the square root of the scan rate ($v^{1/2}$) from 5 to 500 mV/s both with and without DNA, and the y-intercepts are 0 within experimental error (Figure 2, inset). The resolution of the IV/III and III/II couples in Figure 2 is observable for $Ru^{II}(tpy)(bpy)OH_2^{2+}$ only with selected electrodes: activated glassy carbon, edge-oriented pyrolytic graphite (EOPG), and ITO.[10,12,13] In order to ensure that no adsorption of the DNA occurs, we have chosen ITO. At neutral pH, this surface is negatively charged,[14] which we hoped would prohibit adsorption of the DNA polyanion. The linearity of the i_p–$v^{1/2}$ plots shows that there is indeed no adsorption.[15] The slope in DNA (R = [DNA-nucleotide phosphate]/[Ru] = 35) is 37% of the slope in buffer. This reduction in slope is related to the degree of binding, as well shall discuss below.

Another important fact that arises from the electrochemistry of **1** is the observed shift in $E_{1/2}$(III/II) by +26 mV upon the addition of DNA. It has been shown that binding of the metal complex to DNA can bring about a shift in the redox potential if one redox state is more strongly bound than the other.[2] The change in binding constant can be determined according to eq 3, where $E_b^{o\prime}$ and $E_f^{o\prime}$ are the thermodynamic redox potentials

$$E_b^{o\prime} - E_f^{o\prime} = 0.059 \log (K_{Ru(II)}/K_{Ru(III)}) \quad (3)$$

for the bound and free complexes, respectively, and $K_{Ru(II)}/K_{Ru(III)}$ is the ratio of binding constants for the $Ru^{II}OH_2^{2+}$ and $Ru^{III}OH^{2+}$ species. For a limiting shift of +26 mV, we calculate $K_{Ru(II)}/K_{Ru(III)} = 2.76$; i.e., the $Ru^{II}OH_2^{2+}$ form is bound ~3 times more strongly than the $Ru^{III}OH^{2+}$ form. Since the charge on both forms is the same, an increase in electrostatic binding cannot be responsible for the observed change in binding constant upon oxidation. However, ligands containing H-bond donors (i.e. H_2O and NH_3) are known to encourage binding of metal complexes to DNA phosphate groups,[16,17] and $Ru^{II}OH_2^{2+}$ may bind more strongly than $Ru^{III}OH^{2+}$ because of an increased number of H-bond donors for the aqua ligand relative to hydroxo.

In previous work, the measured current for DNA-binding complexes was best fit by a mobile model, where bound and free complexes interconvert on the time scale of a voltammetric scan.[2] The equation describing the current in this model is

$$i_p = BC_t(D_fX_f + D_bX_b)^{1/2} \quad (4)$$

where i_p is the peak current, X_f and X_b are the mole fractions of free and bound metal complex, respectively, D_f and D_b are the free and bound diffusion coefficients, C_t is the total concentration of the complex, and B for a Nernstian reaction at 25 °C is $(2.69 \times 10^5)n^{3/2}Av^{1/2}$, where n is the number of electrons transferred per metal complex, A is the area of the working electrode, and v is the scan rate. For $Co(bpy)_3^{3+}$, D_b is 6.4% of D_f, so when a significant fraction of the metal complex is bound, i_p is greatly

(10) Thorp, H. H.; Brudvig, G. W.; Bowden, E. F. *J. Electroanal. Chem. Interfacial Electrochem.* **1990**, *290*, 293.
(11) Grover, N.; Thorp, H. H. Unpublished results.
(12) Cabaniss, G. E.; Diamantis, A. A.; Murphy, W. R., Jr.; Linton, R. W.; Meyer, T. J. *J. Am. Chem. Soc.* **1985**, *107*, 1845.
(13) Thorp, H. H. *J. Chem. Educ.* **1992**, *69*, 250.
(14) Tret'yakov, N. E.; Filimonov, V. N. *Kinet. Catal.* **1972**, *13*, 735.
(15) Bard, A. J.; Faulkner, L. R. *Electrochemical Methods*; Wiley: New York, 1980.
(16) Gessner, R. V.; Quigley, G. J.; Wang, A. H.-J.; van der Marel, G. A.; van Boom, J. H.; Rich, A. *Biochemistry* **1985**, *24*, 237.
(17) Torres, L. M.; Marzilli, L. G. *J. Am. Chem. Soc.* **1991**, *113*, 4678.

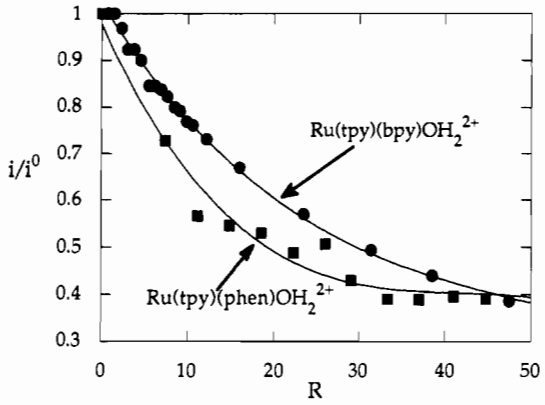

Figure 3. Ratio of current in DNA (i) to current in the absence of DNA (i^0) as a function of R for $[Ru^{II}(tpy)(bpy)OH_2](ClO_4)_2$ (●) and $[Ru^{II}(tpy)(phen)OH_2](ClO_4)_2$ (■). Metal complex concentration: 0.2 mM. Working electrode: ITO. Scan rate: 10 mV/s.

decreased, as seen for **1** in Figure 2.

Using eq 4, it has been possible to determine binding constants for redox-active metal complexes.[2] In these studies, eq 4 is fit to values of the peak current determined as a function of the concentration of DNA-nucleotide phosphate, [NP]. The mole fractions are determined as $X_f = C_f/C_t$ and $X_b = C_b/C_t$, where C_f and C_b are the concentrations of free and bound complex, respectively. The bound concentration is then determined as in eq 5, where s is the size of the binding site in base pairs and K_b

$$C_b = (1/2K_b)[b - (b^2 - (2K_b^2C_t[NP]/s))^{1/2}] \quad (5a)$$

$$b = 1 + K_bC_t + K_b[NP]/2s \quad (5b)$$

is the binding constant for the species present in the bulk solution, in our case $Ru^{II}OH_2^{2+}$. Accurate determinations of the binding constants for $Fe(L)_3^{2+/3+}$ and $Co(L)_3^{3+/2+}$ (L = phen and bpy) have been possible using this method.[2]

In the application of the analysis to **1**, the catalytic cleavage reaction again becomes a difficulty. We can obtain plots of i_p as a function of R similar to those obtained in other systems (Figure 3), which could be fit to determine s and K_b if we knew the values of D_f and D_b. The value for D_f can be determined from the slope of the i_p–$v^{1/2}$ plot in the absence of DNA, according to eq 4, where $X_b = 0$ and $X_f = 1$. From the slope in the absence of DNA (Figure 2, inset), we calculate $D_f = 15.4 \times 10^{-6}$ cm^2/s. In order to measure D_b, we need to make an appropriate measurement at limiting values of R, approximately $R = 1000$.[2] Under these conditions, however, the catalytic enhancement arising from DNA oxidation causes the peak for the Ru(IV/III) couple to overwhelm the Ru(III/II) peak, even in square-wave[3] or differential-pulse polarograms.[15] This can be readily understood in terms of efficient reaction of bound $Ru^{IV}O^{2+}$ with the DNA relative to free $Ru^{IV}O^{2+}$. We have reported that when a majority of the complex is bound, $t_{1/2}$ for cleavage is on the order of a few seconds.[5] Under conditions of very high R, only current from bound species is observed, and the catalytic enhancement is very large. Thus, we cannot determine a diffusion coefficient for the bound III/II couple under these conditions, making exact fitting of the data in Figure 3 impossible with the present system.

Inspection of existing D_b and D_f values shows that, for $Co(bpy)_3^{3+}$, $D_b = 0.064(D_f)$ and $s = 3$ (mobile model, 50 mM ionic strength). In order to estimate K_b for **1**, we will make the approximation that $s = 3$ and the percent reduction in D for binding is the same as in the $Co(bpy)_3^{3+/2+}$ systems, giving $D_b \sim 9.9 \times 10^{-7}$ cm^2/s. We can therefore use the slope of the i_p–$v^{1/2}$ plot in the presence of DNA in Figure 2 to calculate an effective diffusion coefficient at $R = 35$ of $D_{35} = 2.05 \times 10^{-6}$ cm^2/s. From eq 4, we can write this diffusion coefficient in terms of D_f and D_b as

$$D_{35}^{1/2} = (D_fX_f + D_bX_b)^{1/2} \quad (6)$$

which upon rearrangement gives $X_b = 0.93$, or $C_b = 0.185$ mM ($C_t = 0.20$ mM). Simple algebra using eq 5 gives $K_b \sim 15 \times 10^3$ M^{-1} for $Ru^{II}(tpy)(bpy)OH_2^{2+}$, and from eq 3, $K_b \sim 5.4 \times 10^3$ M^{-1} for $Ru^{III}(tpy)(bpy)OH^{2+}$. These values compare favorably with those determined by the complete fitting of the voltammetric data at the same ionic strength on $Co(bpy)_3^{3+/2+}$ ($K_{3+} = 14\,000$ M^{-1}; $K_{2+} = 8400$ M^{-1}), where D_b can be determined experimentally.[2]

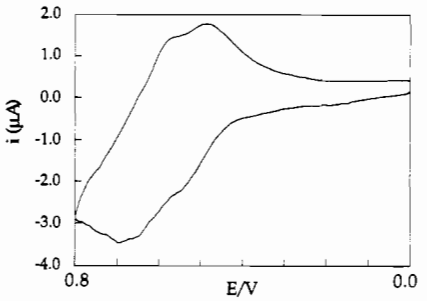

Figure 4. Enlarged cyclic voltammogram of $Ru^{II}(tpy)(bpy)OH_2^{2+}$ in the presence of DNA from Figure 2.

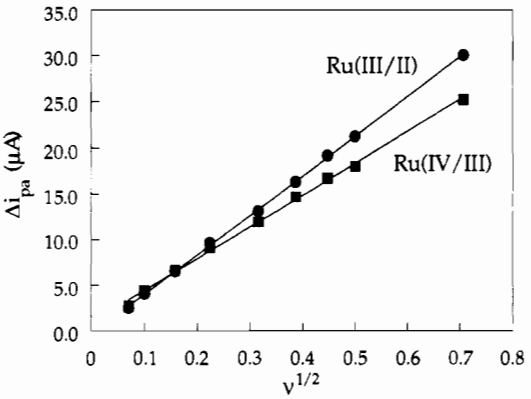

Figure 5. Loss of oxidative current due to addition of DNA as a function of $v^{1/2}$ for Ru(III/II) (●) and Ru(IV/III) (■). $\Delta i_{pa} = i_{pa}$(buffer) – i_{pa}(DNA), where i_{pa}(DNA) is measured at $R = 35$.

$Ru^{II}(tpy)(bpy)OH_2^{2+}$: Cleavage. Figure 4 shows an enlargement of the cyclic voltammogram in the presence of DNA from Figure 2. In addition to the overall decrease in current, a number of other important differences are apparent in comparison to the voltammogram measured in the absence of DNA. The ratio of $i_{pa}(Ru(IV))/i_{pa}(Ru(III))$ is clearly larger in the presence of DNA than in buffer. In light of our observation that $Ru^{IV}O^{2+}$ is quantitatively converted to $Ru^{II}OH_2^{2+}$ during DNA cleavage, this enhancement in the Ru(IV) wave must arise from catalytic oxidation of the DNA.[18] The increased current is particularly apparent in plotting the loss of current brought about by the addition of DNA for $i_{pa}(Ru(IV/III))$ and $i_{pa}(Ru(III/II))$ (Figure 5). The consistently lower values for $\Delta i_{pa}(Ru(IV/III))$ arise from an increase in the Ru(IV/III) current in DNA relative to the Ru(III/II) current in buffer. The plots are linear in $v^{1/2}$, the intercepts are 0 within experimental error, and the enhancement in $i_{pa}(Ru(IV/III))$ persists over the range of scan rates. Since we have observed that cleavage of DNA by $Ru^{IV}(tpy)(bpy)O^{2+}$ leads to the quantitative formation of the starting complex $Ru^{II}(tpy)(bpy)OH_2^{2+}$,[5] we can confidently assign the current enhancement in $i_{pa}(Ru(IV/III))$ to electrocatalytic DNA oxidation. The electrochemical activation of DNA cleavage has been demonstrated in at least three other systems.[19-21]

It is important to note that the experiment samples both free and bound metal complexes, since both are redox-active. In fact, it is apparent from eq 4 that the relative contribution of free and bound metal complex to the overall current can be determined

(18) Nicholson, R. S.; Shain, I. *Anal. Chem.* **1964**, *36*, 706.
(19) Van Atta, R. B.; Long, E. C.; Hecht, S. M.; van der Marel, G. A.; van Boom, J. H. *J. Am. Chem. Soc.* **1989**, *111*, 2722.
(20) Thorp, H. H.; Turro, N. J.; Gray, H. B. *New J. Chem.* **1991**, *15*, 601.
(21) Rodriguez, M.; Kodadek, T.; Torres, M.; Bard, A. J. *Bioconjugate Chem.* **1990**, *1*, 123.

Table I. Electronic Properties and DNA-Binding Parameters of Aquaruthenium Complexes

complex	pK_a(Ru(II))	$E_{1/2}$(Ru(III/II))[a]	$E_{1/2}$(Ru(IV/III))[a]	ref
$Ru^{II}(tpy)(bpy)OH_2^{2+}$ (**1**)	9.7	0.49	0.62	6
$Ru^{II}(tpy)(phen)OH_2^{2+}$ (**2**)	9.6	0.51	0.61	this work
$Ru^{II}(tpy)(tmen)OH_2^{2+}$ (**3**)	10.1	0.45	0.57	this work
$Ru^{II}(bpy)_2(py)OH_2^{2+}$ (**5**)	10.8	0.42	0.54	25a

[a] Potentials in volts vs SSCE, pH 7.

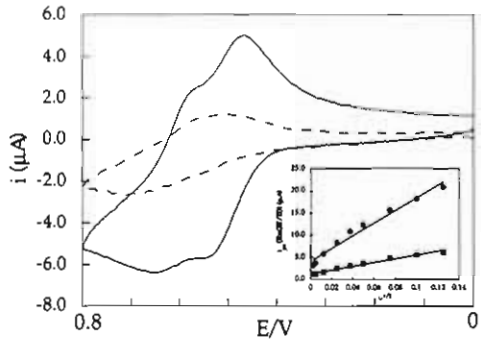

Figure 6. Cyclic voltammograms of 0.2 mM $[Ru^{II}(tpy)(phen)OH_2](ClO_4)_2$ in 0.05 M phosphate buffer, pH 7, with (dashed line) and without (solid line) calf thymus DNA (7 mM nucleotide phosphate). Inset: Plot of i_{pa}(Ru(III/II)) vs $v^{1/2}$ in buffer (●, $R = 0$) and with DNA (■, $R = 35$). Conditions are as in Figure 2.

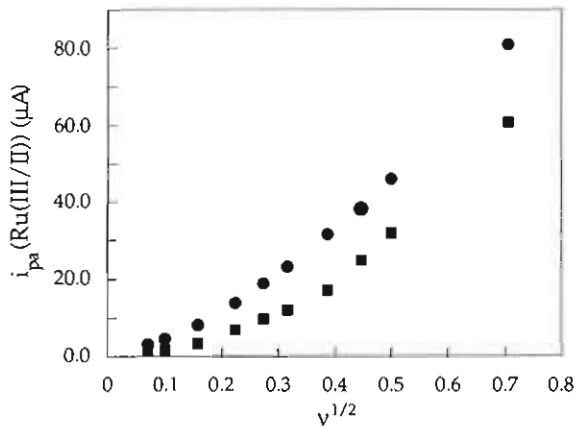

Figure 7. Plot of i_{pa}(Ru(III/II) vs $v^{1/2}$ for $[Ru^{II}(tpy)(phen)OH_2](ClO_4)_2$ without (●, $R = 0$) and with (■, $R = 35$) calf thymus DNA under the same conditions as Figure 5 except with an EOPG working electrode.

as $D_fX_f/(D_fX_f + D_bX_b)$ and $D_bX_b/(D_fX_f + D_bX_b)$, respectively. Using our earlier estimates, this calcualtion shows that at R = 35, 55% of the current is from complex that is free in solution and 45% is from bound complex, even when $X_b = 0.93$. The large amount of current from the free complex is a result of the large value of D_f relative to D_b. This points out a significant limitation of detecting chemical reactions of bound species by electrochemistry. If cleavage only by bound complexes occurs, the voltammetry of the free component will be the same as before the addition of DNA. The experiment then detects the sum of bound and free $Ru^{II}(tpy)(bpy)OH_2^{2+}$, with the free component giving the same wave shape observed in the absence of DNA. Thus, changes in peak potentials and currents brought about by reaction of bound Ru are more subtle than would be expected for a homogeneous electrocatalytic reaction in which binding does not play a role.

$Ru^{II}(tpy)(phen)OH_2^{2+}$. Complex **2** was prepared by the same method as **1**, and its electronic properties are essentially identical (Table I). We have also performed cyclic voltammetric studies of DNA cleavage by **2** and obtain results similar to those for **1** (Figure 6). The linearity of the i_p–$v^{1/2}$ plots (inset) at ITO working electrodes is significant since we have found that substantial adsorption of **2** to edge-oriented pyrolytic graphite (EOPG) does occur both with and without DNA. At ITO, high ionic strength is known to discourage adsorption of cations;[9] we have found that an ionic strength of 50 mM is optimal for voltammetry of **2**. The adsorption of **2** to EOPG electrodes is evident in the i_p–$v^{1/2}$ plots (Figure 7), which show a pronounced upward curvature.[15] Avoiding adsorption is clearly significant in detecting binding accurately, since it appears in Figure 7 that the decrease in current due to addition of DNA is much smaller than at ITO (Figure 6, inset), where no adsorption occurs. This effect is readily understood in terms of adsorption of the electroactive complex to the electrode rather than binding to DNA.

The most striking difference between the voltammetry of **1** and **2** is that the i_p–$v^{1/2}$ plot for **2** (Figure 6, inset) shows that the slope in the presence of DNA is 29% of the slope in buffer. The decrease in slope brought about by the addition of DNA is larger than that for **1**, demonstrating that the phen complex binds more strongly to the DNA, which is expected on the basis of analogous substitutions in related complexes.[2,7] From the slope in the presence of DNA, we can calculate that at $R = 35$, $X_b = 0.98$ compared to $X_b = 0.93$ for **1**. Using the same assumptions as above, we can estimate a binding constant for **2** of $K_b(2) \sim 78 \times 10^3$ M^{-1}, which compares favorably with the value for $Co(phen)_3^{2+}$ of 51×10^3 M^{-1}, determined by complete fitting of voltammetric data.[2] Thus, complex **2** has a significantly greater binding affinity than **1**, which is also evident in the plot of i/i^0 versus R (Figure 3), where the decrease in current for **2** is much more rapid than that for **1**. Careful inspection of cyclic voltammograms of **2** in the presence of DNA reveals results similar to those in Figure 4, with a current enhancement in i_{pa}(Ru(IV/III)) arising from DNA cleavage.

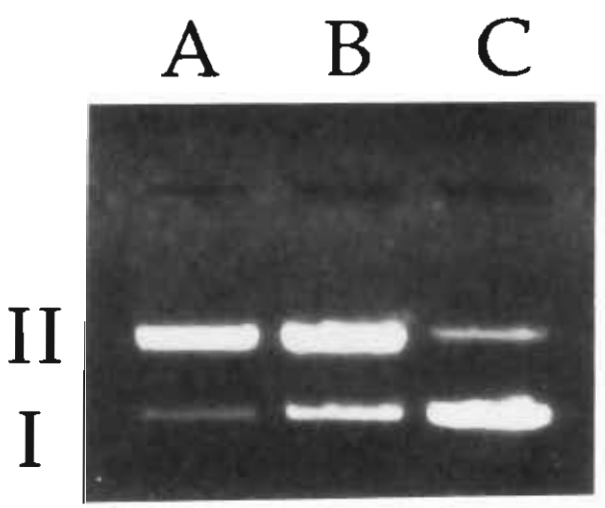

Figure 8. 1% agarose gel showing the results of electrophoresis of 60 μM pSport1 DNA after electrolysis for 1 h in the presence of (A) 20 μM $[Ru^{II}(tpy)(bpy)OH_2](ClO_4)_2$ and (B) 20 μM $[Ru^{II}(tpy)(phen)OH_2](ClO_4)_2$. (C) is a DNA control.

We have reported that controlled potential electrolysis at 0.8 V of solutions of **1** leads to DNA cleavage as monitored by gel electrophoresis.[5] This reaction occurs because the electrolysis generates the active $Ru^{IV}O^{2+}$ form, as shown in eqs 1 and 2. Shown in Figure 8 are the results of a cleavage reaction wherein **1** and **2** were electrolyzed at 0.8 V with pSport1 plasmid DNA for 1 h. Clearly, more extensive conversion of supercoiled (form I) DNA to nicked circular (form II) DNA occurs with **1**. We can understand this observation directly from the above discussion of the binding of the two complexes. Since D_f is much greater than D_b, more of the complex is electrochemically oxidized to Ru(IV) when less of it is bound. Thus, the complex that has a lower binding constant will be oxidized to Ru(IV) most efficiently and will consequently cleave more DNA per unit time than the

Table II. Crystal Data for $Ru^{II}(tpy)(tmen)OH_2^{2+}$

empirical formula	$C_{21}H_{29}N_5O_9RuCl_2$
fw	667.47
cryst dimens	0.60 × 0.40 × 0.04 mm
cryst system	monoclinic
lattice params	a = 15.314 (5) Å
	b = 10.754 (4) Å
	c = 16.150 (8) Å
	β = 96.99 (3)°
	V = 2640 (2) Å^3
space group	$P2_1/c$ (No. 14)
Z	4
D_{calcd}	1.680 g/cm^3
F_{000}	1359.78
μ(Mo Kα)	8.42 cm^{-1}
no. of reflcns measd	total: 6903
	unique: 6070 (R_{int} = 0.010)
function minimized	$\sum w(\|F_o\| - \|F_c\|)^2$
least-squares weights	$1/[\sigma^2(F) + 0.001F^2]$
no. of observns, $I \geq 2\sigma(I)$	3601
$R = \sum\|\|F_o\| - \|F_c\|\|/\|F_o\|$	0.0699
$R_w = [\sum w(\|F_o\| - \|F_c\|)^2/\sum wF_o^2]^{1/2}$	0.0718
goodness of fit indicator	1.587

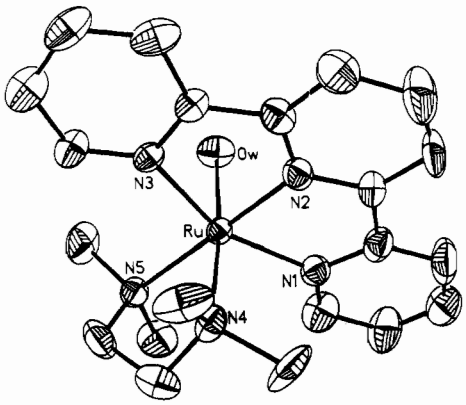

Figure 9. ORTEP diagram of the $Ru^{II}(tpy)(tmen)OH_2^{2+}$ cation (ellipsoids drawn at the 40% probability level; hydrogen atoms omitted for clarity). Selected bond distances (Å) and angles (deg): Ru–Ow, 2.151 (7); Ru–N1, 2.136 (7); Ru–N2, 1.963 (7), Ru–N3, 2.152 (6); Ru–N4, 2.125 (8); Ru–N5, 2.229 (7); N3–Ru–N1, 156.1 (2); N1–Ru–N2, 78.0 (3); N2–Ru–N3, 78.5 (3); N1–Ru–N4, 94.1 (3); N2–Ru–N4, 94.2 (3); N1–Ru–N4, 91.3 (3); N1–Ru–N5, 103.8 (3); N2–Ru–N5, 177.1 (3); N3–Ru–N5, 99.9 (2); N4–Ru–N5, 83.4 (3); N1–Ru–Ow, 89.4 (3); N2–Ru–Ow, 91.5 (3); N3–Ru–Ow, 87.4 (2); Ow–Ru–N4, 173.8 (2).

complex that is more strongly bound and is therefore oxidized to Ru(IV) at a slower rate. On the time scale of controlled potential electrolysis, free Ru(IV) can bind to DNA and undergo reaction, unlike in the voltammetric experiments, where, because of the shorter time scale, DNA cleavage is apparent largely by bound complexes. Thus, the results of the cleavage reaction shown in Figure 8 are consistent with our other cyclic voltammetry experiments in indicating a stronger binding for **2**. Clearly, the dependence of this cleavage efficiency on the binding constant is an important general consideration in designing electrocatalytic systems for DNA cleavage.

Synthesis, Structure, and DNA-Cleavage Properties of $Ru^{II}(tpy)(tmen)OH_2^{2+}$. The functionalization of ethylenediamine ligands bound to Pt(II) has provided new complexes with desirable DNA binding properties.[22] In order to develop more versatile DNA cleavage reagents, we have set out to determine if oxoruthenium(IV) functionalities supported by tertiary amine ligands, which might be more easily functionalized than polypyridines, are effective DNA cleavage agents. We have found that $Ru^{IV}(tpy)(tmen)O^{2+}$ (tmen = *N,N,N′,N′*-tetramethylethylenediamine) is also an effective agent for DNA cleavage. In addition, we have succeeded in obtaining the X-ray crystal structure of its reduced precursor, $Ru^{II}(tpy)(tmen)OH_2^{2+}$ (**3**), which is informative with regard to the electronic structures of this family of complexes.

The structure of **3** determined by X-ray diffraction is shown in Figure 9. The disposition of the tpy ligand, with the central pyridine ring closer than the outer two and an N1–Ru–N3 angle of 156.1°, is very similar to the arrangement seen in $Ru^{II}(tpy)(PMe_3)_2(NO_2)^+$ and $Ru^{VI}(tpy)(O)_2OH_2^{2+}$ (**4**).[23,24] This pattern arises from the steric limitations of the meridonal tpy ligand. The Ru–Ow bond distance is 2.151 Å, the ancillary ligands are not bent away from the Ru–O bond, and there is no lengthening of the Ru–N4 bond relative to the Ru–N5 bond. Thus, there is no evidence for any Ru–O multiple bonding, as expected for

Table III. Atomic Coordinates (×10^4) and Isotropic Thermal Parameters (Å^2 × 10^3) for $Ru^{II}(tpy)(tmen)OH_2](ClO_4)_2$

	x	y	z	U^a
Ru	2574 (1)	6989 (1)	6812 (1)	30 (1)*
N1	1962 (5)	5829 (7)	5835 (4)	42 (2)*
C1	1951 (7)	4579 (9)	5761 (6)	62 (4)*
C2	1511 (8)	3986 (12)	5055 (8)	80 (5)*
C3	1069 (8)	4656 (12)	4450 (7)	74 (5)*
C4	1030 (7)	5915 (13)	4513 (6)	73 (5)*
C5	1497 (6)	6493 (10)	5217 (5)	48 (3)*
N2	1911 (4)	8201 (6)	6074 (4)	40 (2)*
C6	1467 (6)	7834 (9)	5339 (5)	50 (3)*
C7	1065 (7)	8684 (11)	4776 (6)	70 (4)*
C8	1079 (8)	9926 (11)	5002 (7)	78 (5)*
C9	1478 (8)	10322 (10)	5777 (7)	67 (4)*
C10	1905 (6)	9420 (8)	6310 (5)	47 (3)*
N3	2819 (4)	8684 (6)	7510 (4)	34 (2)*
C11	2383 (6)	9646 (7)	7126 (5)	38 (3)*
C12	2387 (7)	10820 (8)	7499 (7)	57 (4)*
C13	2867 (8)	11025 (9)	8265 (7)	62 (4)*
C14	3348 (8)	10090 (9)	8605 (6)	59 (4)*
C15	3307 (7)	8918 (8)	8234 (5)	47 (3)*
N4	3753 (5)	7210 (7)	6256 (4)	45 (3)*
C16	4392 (7)	6283 (11)	6671 (8)	70 (4)*
C17	4277 (6)	6123 (11)	7552 (7)	66 (4)*
N5	3387 (5)	5671 (6)	7647 (4)	41 (2)*
C18	3639 (8)	6881 (13)	5349 (6)	79 (5)*
C19	4150 (7)	8461 (9)	6328 (8)	69 (4)*
C20	3339 (8)	4325 (8)	7446 (7)	63 (4)*
C21	3217 (8)	5772 (10)	8530 (6)	68 (4)*
Ow	1468 (4)	6695 (6)	7493 (4)	51 (2)*
Cl1	3976 (2)	2779 (2)	521 (2)	55 (1)*
O1	3242 (21)	2881 (29)	−63 (21)	193 (12)
O2	3669 (12)	3176 (17)	1303 (11)	96 (6)
O3	4595 (11)	1861 (15)	917 (10)	80 (5)
O4	4726 (15)	3579 (22)	677 (14)	138 (8)
O1′	3853 (16)	2914 (22)	−371 (15)	133 (8)
O2′	3236 (14)	2922 (19)	892 (13)	114 (7)
O3′	4163 (12)	1504 (18)	447 (12)	103 (6)
O4′	4505 (14)	3773 (19)	329 (13)	110 (6)
Cl2	514 (2)	3481 (2)	7662 (2)	60 (1)*
O5	487 (7)	2585 (11)	7013 (7)	117 (3)
O6	−7 (9)	3101 (12)	8245 (9)	158 (5)
O7	1340 (10)	3542 (14)	8124 (9)	171 (5)
O8	343 (13)	4623 (19)	7367 (12)	245 (8)

[a] Asterisk indicates equivalent isotropic U defined as one-third of the trace of the orthogonalized U_{ij} tensor.

Table IV. Ru–Ow and Ru–tpy Bond Lengths (Å) in Related Complexes

bond	$Ru^{II}(tpy)(tmen)OH_2^{2+}$ [a]	$Ru^{VI}(O)_2(H_2O)(tpy)^{2+}$ [b]
Ru–Ow	2.151 (7)	2.128 (25)
Ru–N1	2.136 (7)	2.132 (32)
Ru–N2	1.963 (7)	1.970 (30)
Ru–N3	2.152 (6)	2.076 (29)

[a] This work. [b] Reference 24a.

(22) Bowler, B. E.; Ahmed, K. J.; Sundquist, W. I.; Hollis, L. S.; Whang, E. E.; Lippard, S. J. *J. Am. Chem. Soc.* **1989**, *111*, 1299.

(23) Leising, R. A.; Kubow, S. A.; Churchill, M. R.; Buttrey, L. A.; Ziller, J. W.; Takeuchi, K. J. *Inorg. Chem.* **1990**, *29*, 1306.

(24) (a) Dovletoglou, A.; Adeyemi, S. A.; Lynn, M. H.; Hodgson, D. J.; Meyer, T. J. *J. Am. Chem. Soc.* **1990**, *112*, 8989. (b) Seok, W. K. Ph.D. Thesis, University of North Carolina at Chapel Hill, 1988.

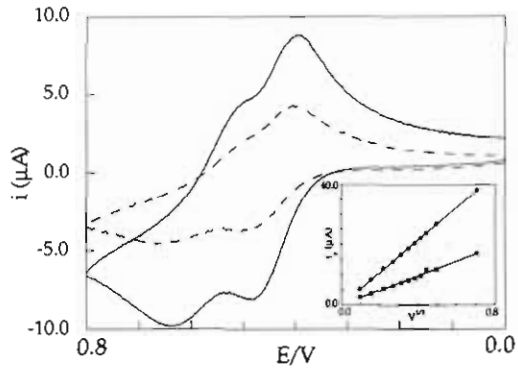

Figure 10. Cyclic voltammograms of 0.2 mM $[Ru^{II}(tpy)(tmen)OH_2](ClO_4)_2$ in 0.05 M phosphate buffer, pH 7, with (dashed line) and without (solid line) calf thymus DNA (7 mM nucleotide phosphate). Inset: Plot of i_{pa}(Ru(III/II)) vs $v^{1/2}$ in buffer (●, $R = 0$) and with DNA (■, $R = 35$). Conditions are as in Figure 1.

this reduced species. In fact, the Ru–N5 bond length is slightly (0.104 Å) longer than the Ru–N4 bond length, which may be a result of the contraction of the Ru–N2 bond due to the steric effect of the tpy ligand. The structure of **1** has also been determined,[24b] and its coordination geometry is closely related to that of **3**.

A significant comparison exists between **3** and **4**. The two complexes both contain Ru–tpy bonds and a Ru–aqua bond, and aside from the stereochemistry, the only difference between the two complexes is the replacement of two Ru–tmen bonds in **2** by multiple Ru=O bonds in **4**. Interestingly, the Ru–aqua and Ru–tpy bond lengths in **3** and **4** are nearly identical (Table IV), *even though the metal centers differ in oxidation state by four electrons*. Meyer and co-workers have discussed the ability of the deprotonation of aqua ligands to stabilize high oxidation states of Ru via formation of multiply bonded oxo groups.[25-28] The comparison in Table IV shows that the presence of two short (1.66 Å) Ru=O bonds in **4** stabilizes Ru(VI) to the extent that the ancillary Ru–aqua and Ru–tpy bond lengths are identical to those found in a complex of Ru(II).

The redox potentials and pK_a values of the coordinated aqua ligand for **3** are given in Table I for comparison with those of **1**, **2**, and $Ru^{II}(bpy)_2(py)OH_2^{2+}$ (**5**).[25a] From the redox potentials, the stabilization of Ru(*III*) and Ru(*IV*) by the (tpy)(tmen) ligand set is greater than **1** and **2** but less than that in **5**. Similarly, the aqua ligand of **3** is more difficult to deprotonate than in **1** and **2** and easier to deprotonate than in **5**. It is satisfying that the redox potentials and the pK_a values are intermediate between those of **1** and **5**. Che and co-workers have reported on these same properties;[8] however, the values obtained by these workers differ somewhat from those we have obtained. The potentials ($E_{1/2}$(III/II) = 0.36 V, $E_{1/2}$(IV/III) = 0.62 V, pH 7) and pK_a (11.7) reported by Che are scattered above, below, and between the values for **1** and **5**.

Figure 10 shows the cyclic voltammetry of **3** with and without DNA at $R = 35$. The i_p–$v^{1/2}$ plots are linear and intersect the origin. From the slope of the plot in the absence of DNA, we can calculate $D_f = 9.8 \times 10^{-6}$, as with **1** and **2**. The slope in DNA is 42% of that in the absence of DNA, demonstrating a lower binding affinity for **3** than **1** or **2**. Using the assumptions above, the mole fraction bound is $X_b = 0.86$, giving a binding constant of $K_b(3) \sim 5.3 \times 10^3\ M^{-1}$.

The electrochemically determined binding parameters for **1**–**3** are set out in Table V for comparison. The relative affinity

Table V. Electrochemical Binding Parameters at $R = 35$

complex	$10^6 D_f$, cm^2/s	$10^6 D_{35}$, cm^2/s	X_b	$10^{-3} K_b$, M^{-1}
$Ru^{II}(tpy)(tmen)OH_2^{2+}$ (**3**)	9.8	1.9	0.86	5.3
$Ru^{II}(tpy)(bpy)OH_2^{2+}$ (**1**)	15	2.1	0.93	15.
$Ru^{II}(tpy)(phen)OH_2^{2+}$ (**2**)	70	6.0	0.98	78.

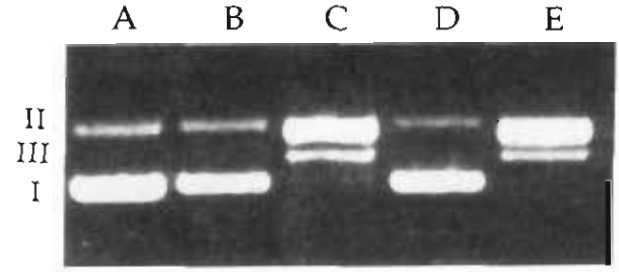

Figure 11. 1% agarose gel showing the results of electrophoresis of 60 μM *ϕX174* DNA (A) in the absence of metal complex, (B) electrolyzed at 0.8 V in the absence of metal complex, (C) electrolyzed at 0.8 V for 2 h in the presence of 40 μM $Ru^{II}(tpy)(tmen)OH_2^{2+}$, (D) incubated with 40 μM $Ru^{II}(tpy)(tmen)OH_2^{2+}$ for 2 h, and (E) incubated with 40 μM $Ru^{IV}(tpy)(tmen)O^{2+}$ for 2 h.

ordering of **3** < **1** < **2** *is consistent with studies of related complexes.*[2,7,29] Complexes containing phen ligands have been shown to interact with DNA by partial intercalation of the phen ligand between the base pairs of the DNA.[7] On the basis of these extensive studies of tris complexes (i.e. $Ru(phen)_3^{2+}$), a plausible binding mode for **2** would involve intercalation of the bidentate phen ligand with the terpyridyl and aqua ligands disposed in the major groove. Simple comparison of the structure of **2** with that of the tris complexes shows that the tpy and aqua ligands can be accommodated in the groove in the same way as two bpy or phen ligands in tris complexes. Thus, the binding affinities may at least partly be a function of the binding affinity of the bidentate ligand. As evident in Figure 1, the degree of extended planarity of the bidentate ligands in the complexes increases in the order **3** < **1** < **2**, the same as the order of binding affinities set out in Table V.

Figure 11 shows the results of DNA cleavage studies conducted with **3** and its oxidized $Ru^{IV}O^{2+}$ form. Electrolysis of **3** at 0.8 V vs Ag/AgCl leads to the formation of the $Ru^{IV}O^{2+}$ form according to eq 7;[8] performing this electrolysis in the presence of

$$Ru^{II}(tpy)(tmen)OH_2^{2+} \rightarrow Ru^{IV}(tpy)(tmen)O^{2+} + 2H^+ + 2e^- \quad (7)$$

supercoiled *ϕX174* DNA leads to cleavage, which is evident in the conversion of supercoiled (form I) DNA to nicked circular (form II) DNA (lane C). Incubation with the $Ru^{IV}O^{2+}$ form also induces cleavage (lane E), but no cleavage is observed upon electrolysis at 0.8 V in the absence of metal complex (lane B) or incubation with **3** (lane D).

The results of Figure 11 are somewhat unusual in that we observe a significant amount of linear (form III) DNA in lanes C and E. Densitometry shows that linear DNA accounts for ~20% of the observed cleavage. We observe form III DNA both in the electrocatalytic reaction (lane C) and in the thermal reaction (lane E). This is in contrast to our earlier results for **1**, where we do not observe a significant form III band under identical conditions. In order to obtain form III DNA, two cleavage events must occur on different strands less than 12 base pairs apart.[30] Importantly, we observe no form III DNA under electrocatalytic conditions with **1**, even when running the electrolysis for 4 times the period required to convert all of the form I DNA to form II. The observation of a substantial amount of form III DNA solely upon switching a bpy ligand to tmen suggests that further study

(25) (a) Moyer, B. A.; Meyer, T. J. *Inorg. Chem.* **1978**, *100*, 3601. (b) Binstead, R. A.; Meyer, T. J. *J. Am. Chem. Soc.* **1987**, *109*, 3287. (c) Thompson, M. S.; Meyer, T. J. *J. Am. Chem. Soc.* **1982**, *104*, 4106.
(26) Pipes, D. W.; Meyer, T. J. *J. Am. Chem. Soc.* **1984**, *106*, 7653.
(27) For more comprehensive reviews, see: Nugent, W. A.; Mayer, J. M. *Metal-Ligand Multiple Bonds*; Wiley Interscience: New York, 1988. Meyer, T. J. *J. Electrochem. Soc.* **1984**, *131*, 221C. Holm, R. H. *Chem. Rev.* **1987**, *87*, 1401.
(28) Takeuchi, K. J.; Samuels, G. J.; Gersten, S. W.; Gilbert, J. A.; Meyer, T. J. *Inorg. Chem.* **1983**, *22*, 1407.
(29) Fleisher, M. B.; Waterman, K. C.; Turro, N. J.; Barton, J. K. *Inorg. Chem.* **1986**, *25*, 3549.
(30) Kishikawa, H.; Jiang, Y.-P.; Goodisman, J.; Dabrowiak, J. C. *J. Am. Chem. Soc.* **1991**, *113*, 5434.

may provide insight into the factors controlling multiple, proximal cleavage events on different strands.[31] Further experimentation will show whether this linearization is a result simply of the greater efficiency of cleavage by **3** or a special mechanism not available to **1** and **2**. In either event, it appears that complex **3** will provide a synthetic entry point into functionalized oxoruthenium(IV) cleavage agents with a wide range of DNA-binding properties and cleavage reactivity.

Conclusions

We have shown that cyclic voltammetry of **1-3** can be used to detect the noncovalent binding of the $Ru^{II}OH_2^{2+}$ forms to DNA and the cleavage of DNA by $Ru^{IV}O^{2+}$. The results show stronger binding of **2** by a factor of 5 relative to **1**, which binds more strongly than **3** by a factor of 3. This observation is consistent with studies on related complexes conducted using both electrochemical[2] and biochemical methods,[7] and we have observed stronger binding of **2** in a variety of biochemical experiments.[11] In the experiments described here, the stronger binding is evident in a larger decrease in current upon addition of the same amount of DNA to solutions that are the same concentration in metal complex. This decrease can be used to estimate the binding affinity. We have found that ITO working electrodes at 50 mM ionic strength allow for the accurate detection of binding in the absence of adsorption of the complex to the electrode; however, substantial adsorption of **2** to EOPG prohibits extraction of binding information using this electrode.

The electrocatalytic cleavage of DNA by $Ru^{IV}O^{2+}$ is apparent in a current enhancement in the IV/III couple. The detection of this catalytic current is complicated by the large contribution of current from quasi-reversible oxidation of free complex to the measured voltammogram, even in solutions where >90% of the complex is bound. Analysis of the difference in current for the IV/III and III/II couples upon addition of DNA (Figure 5) is a straightforward method for qualitatively assessing the degree of current enhancement. The efficiency of DNA cleavage upon controlled potential electrolysis is strongly influenced by the degree of binding of the complex to the DNA. Stronger binding of the complex in the $Ru^{II}OH_2^{2+}$ form leads to lower efficiency of electrocatalytic cleavage, because the active $Ru^{IV}O^{2+}$ form is generated at a slower rate.

Acknowledgment. We thank Professor E. F. Bowden for experimental assistance and helpful discussions. H.H.T. thanks the National Science Foundation for a Presidential Young Investigator Award (CHE-9157411), the David and Lucile Packard Foundation for a Fellowship in Science and Engineering, the Camille and Henry Dreyfus Foundation for a New Faculty Award, and the North Carolina Biotechnology Center for an Academic Research Initiation Grant. We also thank Professor F. M. Hawkridge for a gift of ITO.

Registry No. **1**, 20154-63-6; **2**, 101241-02-5; **3**, 127714-17-4; **3**$(ClO_4)_2$, 127714-24-3; Ru^{III}(tpy)(phen)$(OH)^{3+}$, 81971-63-3; Ru^{III}(tpy)(tmen)$(OH)^{3+}$, 140661-30-9; Ru^{IV}(tpy)(phen)O^{2+}, 98542-34-8; Ru^{IV}(tpy)(tmen)O^{2+}, 127714-19-6; Ru^{IV}(tpy)(bpy)O^{2+}, 73836-44-9.

Supplementary Material Available: Tables giving a summary of the crystal data and details of the X-ray data collection, atomic fractional coordinates, thermal parameters, and complete interatomic distances and angles and a drawing of **3**$(ClO_4)_2$ showing the complete atomic labeling (10 pages); a listing of observed and calculated structure factors (36 pages). Ordering information is given on any current masthead page.

(31) Basile, L. A.; Barton, J. K. *J. Am. Chem. Soc.* **1987**, *109*, 7548.

Contribution from the Department of Chemistry and Biochemistry, University of Colorado, Boulder, Colorado 80309

Semiquinone Imine Complexes of Ruthenium. Coordination and Oxidation of the 1-Hydroxy-2,4,6,8-tetra-*tert*-butylphenoxazinyl Radical

Samaresh Bhattacharya and Cortlandt G. Pierpont*

Received December 2, 1991

Reactions between $Ru(PPh_3)_3Cl_2$ and the 1-hydroxy-2,4,6,8-tetra-*tert*-butylphenoxazinyl radical (HPhenoxSQ) have been investigated. Stoichiometric reactions carried out under inert conditions with ratios of 1:1 and 1:2 for $Ru(PPh_3)_3Cl_2$ to HPhenoxSQ gave as products $Ru(PPh_3)_2Cl_2$(PhenoxSQ) and $Ru(PPh_3)Cl$(PhenoxSQ)$_2$, respectively. The complexes have been characterized spectrally, electrochemically, and structurally ($Ru(PPh_3)_2Cl_2$(PhenoxSQ), monoclinic, $P2_1/n$, a = 19.570 (6) Å, b = 14.652 (4) Å, c = 19.999 (7) Å, β = 91.65 (3)°, V = 5732 (3) Å^3, Z = 4, R = 0.032; $Ru(PPh_3)Cl$(PhenoxSQ)$_2$, monoclinic, $P2_1/c$, a = 10.228 (2) Å, b = 27.775 (8) Å, c = 23.656 (9) Å, β = 97.77 (2)°, V = 6658 (3) Å^3, Z = 4, R = 0.045). $Ru(PPh_3)_2Cl_2$(PhenoxSQ) is diamagnetic due to strong spin coupling between the radical and the $S = {}^1/_2$ metal ion; $Ru(PPh_3)Cl$(PhenoxSQ)$_2$ has a single unpaired electron. 2,4,6,8-Tetra-*tert*-butylphenoxazin-1-one (PhenoxBQ) has been characterized structurally (monoclinic, $P2_1/c$, a = 11.547 (4) Å, b = 17.659 (6) , c = 13.579 (3) Å, β - 105.92 (2)°, V = 2662 (1) Å^3, Z = 4, R = 0.063) to give metrical parameters for the benzoquinone imine ligand in its unreduced form. PhenoxBQ has also been characterized electrochemically. It undergoes two reversible reductions at potentials that are shifted negatively relative to related benzoquinone ligands. Increased energy of the PhenoxBQ π^* level relative to the energy of a benzoquinone antibonding electronic level results in an important difference in the order of energies of complex electronic levels. Reduction of $Ru(PPh_3)Cl$(PhenoxSQ)$_2$ occurs at the metal to give a Ru(II) product, while reduction of corresponding semiquinone complexes occurs at the quinone ligands. The electrochemical potential for reduction of $Ru(PPh_3)Cl$(PhenoxSQ)$_2$ is −1.02 V (Fc/Fc$^+$) and in its reduced form the complex is strongly nucleophilic. When the reaction between $Ru(PPh_3)_3Cl_2$ and HPhenoxSQ is carried out in air at a 1:2 stoichiometry, the product is a Ru(III) complex containing an oxidized form of PhenoxBQ. Two oxygen atoms and one hydroxyl group have been added to the coordinated PhenoxSQ ligand with ring-opening and cyclization leading to formation of a substituted dihydrofuran ring. The resulting complex $Ru(PPh_3)Cl$(PhenoxSQ)(OxPhenox) contains three chiral centers, two at carbon atoms and the third at the metal. Both oxygen addition and cyclization occur stereoselectively to give a single diastereomer. $Ru(PPh_3)Cl$(PhenoxSQ)(OxPhenox) has been characterized spectrally and structurally (monoclinic, $P2_1/c$, a = 19.092 (6) Å, b = 16.018 (7) Å, c = 24.889 (10) Å, β = 111.74 (3)°, V = 7070 (5) Å^3, Z = 4, R = 0.060). A mechanistic scheme is proposed for its formation by the reaction of reduced $Ru(PPh_3)Cl$(PhenoxSQ)$_2^-$, formed initially in the reaction, with molecular oxygen.

Introduction

Developments in the coordination chemistry of quinone ligands over the past 15 years have provided a number of surprising results. A general result that was unanticipated at the outset of this project is the exceptional stability and ubiquity of radical semiquinone complexes with transition-metal ions. The physical and chemical properties of these complexes have been a focus of interest. Magnetic spin coupling between a paramagnetic metal ion and the radical ligand is a specific physical property that has been found to occur characteristically for the semiquinone complexes.[1]

0020-1669/92/1331-2020$03.00/0